Environmental Pollution 234 (2018) 726–734

Contents lists available at ScienceDirect

Environmental Pollution

journal homepage: www.elsevier.com/locate/envpol

Cation-induced coagulation of aquatic plant-derived dissolved organic matter: Investigation by EEM-PARAFAC and FT-IR spectroscopy☆

Shasha Liu [a, b], Yuanrong Zhu [b], Leizhen Liu [c], Zhongqi He [d], John P. Giesy [e], Yingchen Bai [b], Fuhong Sun [b, *], Fengchang Wu [b]

[a] Key Laboratory of Marine Environment and Ecology, Ministry of Education, Ocean University of China, Qingdao 266100, China
[b] State Key Laboratory of Environment Criteria and Risk Assessment, Chinese Research Academy of Environmental Sciences, Beijing 100012, China
[c] Faculty of Geographical Science, Beijing Normal University, Beijing 100875, China
[d] USDA-ARS Southern Regional Research Center, 1100 Robert E Lee Blvd, New Orleans, LA 70124, USA
[e] Department of Veterinary Biomedical Sciences and Toxicology Centre, University of Saskatchewan, Saskatoon, Saskatchewan S7N 5B3, Canada

ARTICLE INFO

Article history:
Received 18 September 2017
Received in revised form
10 November 2017
Accepted 23 November 2017

Keywords:
Plant-derived dissolved organic matter (DOM)
Metal ions
Coagulation
Fluorescence excitation emission matrices-parallel factor (EEM-PARAFAC) analysis
Fourier transform infrared (FT-IR) spectroscopy

ABSTRACT

Complexation and coagulation of plant-derived dissolved organic matter (DOM) by metal cations are important biogeochemical processes of organic matter in aquatic systems. Thus, coagulation and fractionation of DOM derived from aquatic plants by Ca(II), Al(III), and Fe(III) ions were investigated. Metal ion-induced removal of DOM was determined by analyzing dissolved organic carbon in supernatants after addition of these metal cations individually. After additions of metal ions, both dissolved and coagulated organic fractions were characterized by use of fluorescence excitation emission matrix-parallel factor (EEM-PARAFAC) analysis and Fourier transform infrared (FT-IR) spectroscopy. Addition of Ca(II), Fe(III) or Al(III) resulted in net removal of aquatic plant-derived DOM. Efficiencies of removal of DOM by Fe(III) or Al(III) were greater than that by Ca(II). However, capacities to remove plant-derived DOM by the three metals were less than which had been previously reported for humic materials. Molecular and structural features of plant-derived DOM fractions in associations with metal cations were characterized by changes in fluorescent components and infrared absorption peaks. Both aromatic and carboxylic-like organic matters could be removed by Ca(II), Al(III) or Fe(III) ions. Whereas organic matters containing amides were preferentially removed by Ca(II), and phenolic materials were selectively removed by Fe(III) or Al(III). These observations indicated that plant-derived DOM might have a long-lasting effect on water quality and organisms due to its poor coagulation with metal cations in aquatic ecosystems. Plant-derived DOM is of different character than natural organic matter and it is not advisable to attempt removal through addition of metal salts during treatment of sewage.

1. Introduction

Dissolved organic matter (DOM), defined as a complex, incompletely characterized mixture with a variety of aliphatic and aromatic compounds, is present ubiquitously in aquatic systems (Swietlik and Sikorska, 2006; Wu and Xing, 2009). Due to the intrinsic negative charges present in most DOM, they can bind metal ions, which would either enhance or reduce mobility of metal cations in aquatic systems by forming dissolved or insoluble complexes (Fu et al., 2007; Kaiser, 1998; Tipping, 2002). In addition, formation of insoluble complexes of metal-DOM, called coagulation, could influence chemical composition and activity of DOM in aquatic environments.

Composition and characteristics of DOM are key factors in control of its interactions with metal cations, including sorption and coagulation (Kaiser, 1998; Riedel et al., 2012). For example, the hydrophobic fraction was selectively decreased after interaction with added Ca(II), Al(III), or Fe(III), which was possibly due to the formation of insoluble DOM-metal complexes (Kaiser, 1998). Aromatic and phenolic carbon of a purified humic acid decreased significantly after cation-induced coagulation by Al(III) or Fe(III) (Christl and Kretzschmar, 2007). In addition, types of metal ions are also an important factor that influences chemical fractionation of

☆ This paper has been recommended for acceptance by B. Nowack.

* Corresponding author. No. 8 Dayangfang, BeiYuan Road, ChaoYang District, Beijing 100012, China.
E-mail address: sunfhiae@126.com (F. Sun).

https://doi.org/10.1016/j.envpol.2017.11.076
0269-7491/

DOM in cation-induced coagulation due to their various binding affinities for special compounds or functional groups in DOM (Christl and Kretzschmar, 2007). It was reported that Ca(II) did not show any preference for distinct molecular fractions, while Fe(III) and Al(III) preferentially removed the most oxidized compounds in DOM (Riedel et al., 2012). Also, calculations based on NICA-Donnan parameters revealed that under experimental conditions, Ca(II) mainly binds to carboxylic-like functional groups, while Fe(III) and Al(III) were also bound to phenolic-like functional groups (Milne et al., 2003). These observations provide valuable insights into the principal mechanisms of coagulation. However, these studies are mainly focused on natural waters or commercial humic acids (Gone et al., 2009; Riedel et al., 2012; Zhu et al., 2014), limited studies have been conducted on DOM derived from autochthonous materials (McIntyre and Guéguen, 2013). Eutrophication caused by mobilization and transport of plant nutrients through anthropogenic activity has caused excessive growth of emergent and submerged macrophyte in shallow freshwater lakes. Thus, due to its large quantities of biomass, plant-derived DOM constitutes one of the most important contributors to pools of DOM in lakes (Findlay and Sinsabaugh, 2003). Additionally, due to their limited degradation history compared with natural DOM that undergoes multi-decomposition processes, plant-derived DOM has unique molecular compositions (Liu et al., 2016a; Zhang et al., 2013). Therefore, studies of coagulation of plant-derived DOM by cations and their difference from other types of organic matters were needed to fill this gap in knowledge of DOM, which would further our understanding of the environmental behavior of DOM in aquatic systems.

Excitation-emission matrix (EEM) fluorescence spectroscopy, which could identify humic-like and protein-like organic compounds, provides important information on characteristics of DOM without requiring tedious pretreatment or fractionations (Cuss and Guéguen, 2015; Wu et al., 2004a, 2004b, 2003; Zhao et al., 2013). Fluorescence intensities of EEMs, given as a function of emission (Em) and excitation (Ex) wavelength are typically used to characterize DOM and often assessed by visual inspection. EEM has been used to evaluate efficiency of removal of organic matter during treatment of water by coagulation-flocculation (Gone et al., 2009; Zhu et al., 2014). In order to make a quantitative comparison between EEMs of samples, multivariate statistical techniques have been used extensively (Ishii and Boyer, 2012). One of the multivariate approaches, parallel factor (PARAFAC) analysis, allows EEMs to be classified into fluorescent components, which is useful for assessment of composition, distribution and dynamics of DOM from aquatic environments (Baghoth et al., 2011; Murphy et al., 2011; Osburn et al., 2012).

Fourier transform infrared (FT-IR) spectroscopy can provide additional information on functional groups present in organic matters (Bernier et al., 2013). Thus, combined utilization of EEM-PARAFAC and FT-IR can provide complementary information on cation-induced coagulation of aquatic plant-derived DOM in aquatic systems. Hence, in this study, molecular compositions of "precipitable" and "non-precipitable" fractions of plant-derived DOM were investigated by use of a combination of EEM-PARAFAC and FT-IR spectroscopy. Objectives of this study were to: (1) assess removal of DOM during coagulation-flocculation with metal ions Ca(II), Al(III) or Fe(III); and (2) explore molecular and structural characteristics of the aquatic plant-derived DOM during and post cation-induced coagulation.

2. Materials and methods

2.1. Plant-derived DOM

Based on results of previous studies, molecular characteristics of aquatic plants were basically uniform for emergent, floating and submerged plants in lakes (Liu et al., 2016a, 2016b, 2017). Thus, one species of water oats (*Zizania caduciflora* Turcz., Gramineae) was chosen as a representative aquatic plant present in lakes to study the interaction of plant-derived DOM with metal ions. Collection and preparation of samples were carried out as described in detail previously (Liu et al., 2016a). Briefly, whole fresh plant biomass was washed and dried at 60 °C until a constant mass. After drying, plants were ground to pass through a 1-mm sieve and stored in an airtight desiccator. Extraction of DOM was carried out by use of a 30:1 (mL/g) Mili-Q water to ground plant biomass ratio. After 18 h of shaking at 22 °C, the suspension was allowed to stand for 1 h and passed through 0.45-μm glass fiber filters.

Dissolved organic carbon (DOC) was measured by a multi N/C 3100 analyzer (Jena, Germany). The original plant-derived DOM had a DOC concentration of 110 mM carbon. In order to better simulate concentration of DOC in natural waters with vast quantities of plant decomposition, original plant-derived DOM was diluted until 2.2 mM carbon (the diluted extracts was used as the raw plant-derived DOM) in studies of coagulation. The pH of final dilute solution was 5.0.

2.2. Metal additions and coagulation

Concentrations of metals in dilute, plant-derived DOM, measured by inductively coupled plasma-optical emission spectroscopy (ICP-OES, OPTIMA 8000DV), were: 6.3 μmol Ca(II), 6.5 μmol Al(III), 18.6 μmol Fe(III). Since perchlorate contributions to absorbance spectra of DOM were reportedly small, stock solutions of metal ions were prepared using their perchlorate salts $Ca(ClO_4)_2$, $Al(ClO_4)_3$, and $Fe(ClO_4)_3$ (Yan et al., 2013; Yan and Korshin, 2014). Additions of metal salts were carried out by adding required volumes of stock into 100 mL raw plant-derived DOM. Final concentrations of metals in solutions were 0.4, 1.0, 2.0, 4.0 and 10.0 mM. Final pH of prepared solutions was adjusted to 4.5 by adding NH_3 solution or $HClO_4$ to avoid pH-dependent solubility effects (Amirsardari et al., 1997; Nierop et al., 2002). Prepared solutions were shaken for 48 h at room temperature (22 °C) to reach full equilibrium. After that, solutions were allowed to stand for 4 h and then passed through 0.45-μm membrane filters. Aliquots of supernatants were used for measurement of DOC, ultraviolet (UV) absorbance spectra and fluorescence spectra. Remaining supernatants and coagulates were freeze-dried, and then preserved in a desiccator at room temperature for FT-IR analysis. Experiments were conducted in triplicate.

2.3. Spectroscopic measurements

Filtered samples were analyzed for Ultraviolet (UV) absorbance and fluorescence analysis. UV absorbance spectra from 200 to 600 nm were measured with a UV-vis spectrophotometer (Agilent 8453), using a 1-cm path length cell. In order to prevent any inner filter effect, solutions were diluted to a UV absorbance at 260 nm of 0.1 using purified water (Ohno and He, 2011).

Fluorescence measurements were made by an F-7000 fluorescence spectrophotometer (Hitachi, Japan). Excitation and emission wavelength ranges were set from 200 to 450 nm and 250–600 nm, respectively. Excitation and emission increments were 5 nm with a slit of 10 nm for both Ex and Em. Scan speed was set at 1200 nm/min. Photomultiplier detector voltage was fixed at 400 V. EEMs were measured using 1-cm path length quartz cells. In order to remove Raman and Rayleigh scatter from fluorescence spectra, fluorescence of a blank solution consisting of purified water was subtracted from the 3D scan. Variation in the lamp light intensity was measured by recording the Raman peak area for deionized

water at an excitation wavelength of 350 nm (emission wavelength range: 375–425 nm) each day the instrument was used (Lawaetz and Stedmon, 2009). Results of Raman peak area for the analysis day were used to normalize results of fluorescence intensity. Parallel factor (PARAFAC) analysis was utilized to examine EEMs following the tutorial guidelines in literature (Stedmon and Bro, 2008). The fluorescence results in EEM-PARAFAC components were reported as Raman Units (R.U.).

FT-IR spectra of both freeze-dried supernatants and coagulates were measured by a Bruker Vertex 70 spectrometer. The analysis was conducted in the mid-infrared region from 4000 cm^{-1} to 400 cm^{-1} with a resolution of 4 cm^{-1}.

3. Results and discussion

3.1. Removal of DOM

Concentrations of DOC in supernatants decreased with addition of metal cations Ca(II), Al(III) and Fe(III) (Fig. 1). Approximately 31% and 16.7% of DOC were removed, respectively when total concentrations of Fe(III) or Al(III) were 10 mM, but only 6% of DOC was removed by the same concentration of Ca(II). These observations suggested that addition of metal cations Ca(II), Al(III), and Fe(III) definitely induced the coagulation and removal of DOM. And the removal capabilities for DOM were much greater by Fe(III) and Al(III) than that by Ca(II). It has been reported that Ca(II) is weakly complexed with DOM, whereas Fe(III) and Al(III) are more strongly associated with DOM (Kerndorff and Schnitzer, 1980; Nierop et al., 2002; Tipping, 2002). Thus, observations made during this study were consistent with previously reported results. However, efficiency of removal of these metal cations for plant-derived DOM is quite different from those DOM from other sources. Addition of 0.4 mM Al(III) or 0.5 mM Fe(III) could remove 90% of DOM (prepared by a purified humic acid) at pH 4, but 5 mM Ca(II) only could remove 84% of DOM at pH 6 (Christl and Kretzschmar, 2007). Additionally, Riedel et al. (2012) indicated that Fe(III) precipitated most of the DOM (up to 85%), followed by Al(III) (74%). Addition of Ca(II) resulted in only small amounts of (up to 18%) of water-soluble DOM extracted from commercially available peat to be removed. In the current study, Fe(III), Al(III), or Ca(II) all removed much less DOM than that previously reported values when similar ratios of DOC/metal and pH were used (Christl and Kretzschmar, 2007; Riedel et al., 2012). It was thus, hypothesized that chemical structures of DOM are likely the key factor affecting coagulations observed differently. To confirm the assumption, plant-derived DOM in this work was further characterized by multi-spectroscopic techniques. In addition, molecular compositions of the "precipitable" and "non-precipitable" fractions of plant-derived DOM were characterized by EEM-PARAFAC and FT-IR spectroscopy.

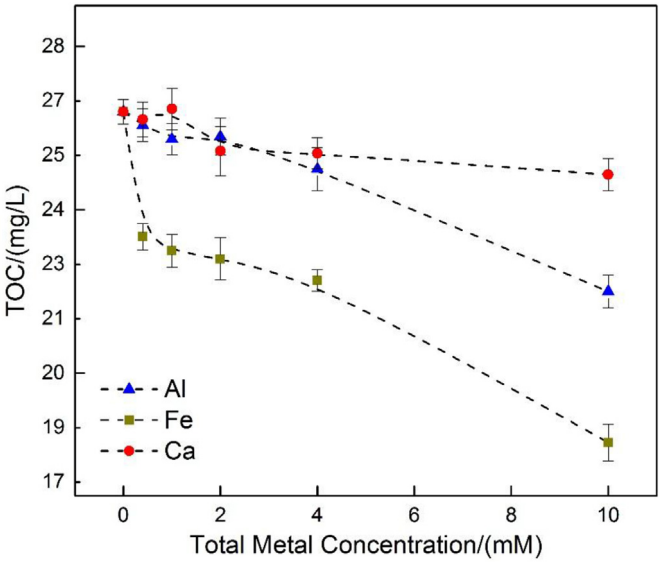

Fig. 1. Concentrations of DOC in the supernatants of plant-derived DOM extracts incubated in the presence of metal ions. Error bars represent standard deviations; n = 3.

3.2. Spectral characterization of the raw plant-derived DOM

Based on the traditional EEMs 'peak picking' (Coble, 1996), two humic-like peaks (peaks A and C) and two protein-like peaks (peaks T1 and T2) were detected in plant-derived DOM (Fig. S1). One humic-like fluorescence peak was in the visible region (peak C; Ex/Em = 300–315 nm/420–430 nm) and the other was in ultraviolet region (peak A; Ex/Em = 230–240 nm/420–440 nm). Peaks A and C are generally considered to be associated with humic-like (mainly humic and fulvic acids) compounds derived from breakdown of plant materials (Coble, 1996). The presence of these two peaks has always been attributed to phenolic, carboxylic acids and carbonylic compounds in DOM (Senesi, 1990). The protein-like fluorescence peaks were observed at both a long excitation wavelength (peak T1; Ex/Em = 265–275 nm/330–350 nm) and a short excitation wavelength (peak T2; Ex/Em = 215–225 nm/330–360 nm). These two protein-like fluorescence peaks (Peaks T1 and T2) were considered to be associated with the tryptophan-like substances (Baker, 2001; Baker and Inverarity, 2004; Chen et al., 2003; Yamashita and Tanoue, 2003). These observed fluorescence peaks have also been identified in other leachates such as algae exudation (Li et al., 2008; McIntyre and Guéguen, 2013; Romera-Castillo et al., 2011; Stedmon and Markager, 2005), marine phytoplankton cultures (Castillo et al., 2010), and bacterial extracellular polymeric substances (He et al., 2006; Olk et al., 2000).

Spectral peak features of 3D EEM fluorescence were quantitatively separated into four fluorescence components by use of half-split analysis of PARAFAC (Fig. 2). These fluorescence components were assigned based on previous reports (Agnelli et al., 2000; Castillo et al., 2010; Duarte et al., 2005). Component 1, which was classified as hydrophobic matter that belongs to the high molecular weight aromatic organic compounds, had a dominant peak with maximum excitation and emission values of 250/440 nm and a second broad peak at Ex/Em = 290–345/440 nm. Component 2 was classified as protein-like compounds, which had a primary and secondary excitation peak around 275 nm and 220 nm, respectively, with a single emission peak around 350 nm. Component 3 had two dominant peaks around Ex/Em = 220 nm/330–350 nm and 220 nm/400–430 nm, also with two minor bands centered around Ex/Em = 270 nm/300–350 nm and 270 nm/400–430 nm. This peak resembled to tryptophan-like components in undenatured protein structures and could be also contributed by polyphenolic materials (Cuss and Guéguen, 2015; He et al., 2014). Component 4 was classified as fulvic-like substances, which had a primary and secondary excitation peak occurring around 235 nm and 325 nm, with a single emission peak around 400 nm. Plant-derived DOM consisted of 26% component 1, 30% component 2, 23% component 3 and 21% component 4 (Fig. 2).

Functional groups of carbon in raw plant-derived DOM were further characterized by FT-IR spectroscopy. Six typical peaks or bands centered at 3283 cm^{-1}, 2928 cm^{-1}, 1626 cm^{-1}, 1402 cm^{-1}, 1310 cm^{-1}, and 1038 cm^{-1} were observed from the FT-IR spectrum of raw plant-derived DOM (Fig. 3). The broad band around 3283 cm^{-1} was assigned to N-H stretching from amide/amino acid

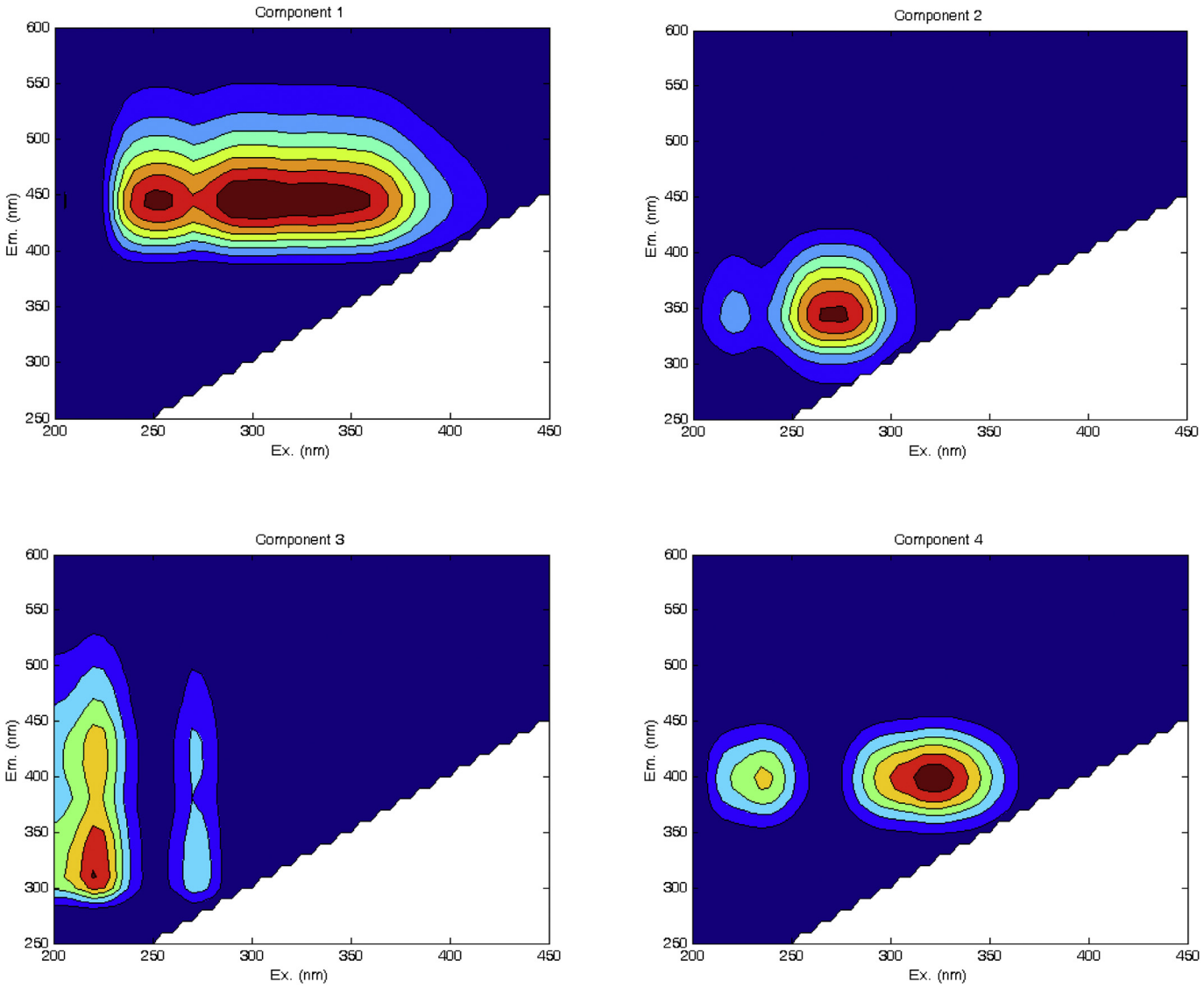

Fig. 2. Spectral features and the relative abundance of fluorescence components of plant-derived DOM separated by EEM-PARAFAC.

or O-H bond stretching from phenols, alcohols, carboxylic acids, and/or other substances which contains hydroxyl groups (Francioso et al., 1996; Kang et al., 2002; Lguirati et al., 2005). The minor band at 2928 cm^{-1} corresponds to C–H stretching of methyl and methylene groups of aliphatic chains (Duarte et al., 2005; He et al., 2006; Olk et al., 2000). The sharp band at 1600 cm^{-1} or so was assigned to aromatic C=C vibration, olefinic C=C bonds, symmetric stretching of COO^- groups, and H-bonded C=O of conjugated ketones (Francioso et al., 1996; Olk et al., 2000). The minor peak at 1402 cm^{-1} was due to phenolic OH and aliphatic C-H groups (Agnelli et al., 2000). A minor band at 1310 cm^{-1} was assigned to C-N stretch of aromatic primary and secondary amines. The strong band at 1038 cm^{-1} was attributed to alcoholic and polysaccharide C-O stretching, silicate vibrations or phosphorus (P) compounds (Agnelli et al., 2000; Francioso et al., 1996; He et al., 2006). As a result, all groups of C-H and phenols at 1402 cm^{-1}, C–H stretching vibration at 2928 cm^{-1} and the lack of COO^- at 1710-1725 cm^{-1} indicated that plant-derived DOM was characterized by polysaccharides, amino acids, and phenols/alcohols with few humic substances.

3.3. Effects of additions of metal cations on spectral features of plant-derived DOM

Changes of the proportional distribution of fluorescence components after cation-induced coagulation could be used to detect the molecular fractionation of plant-derived DOM through selective binding and coagulation by metal cations (Fig. 4). Addition of Ca(II) decreased the percentage of component 1 and 4, and the percentage of these two components continuously decreased with the increasing addition of Ca(II). This result suggested that Ca(II) was easier to combine with humic-like and fulvic-like hydrophobic matters which belong to high molecular weight aromatic organic matters. This observation is consistent with a previous report that Ca(II) has stronger affinity for binding to humic acids (He et al., 2003). With increasing concentrations of Fe(III) or Al(III), the relative abundance of component 1 was continuously decreased. While the relative abundance of component 2 decreased continuously with the increasing addition of Fe(III) and Al(III) when their concentration exceeded 0.4 mM. Thus, Fe(III) and Al(III) might have similar binding sites on DOM, and they were readily to bind with humic-like, fulvic-like and aromatic protein-like components. It is worth while noting that the so-called protein-like fluorescence peak was not only derived from proteinaceous materials but also from phenolic moieties such as tannins (Hernes et al., 2009; Maie et al., 2007). Indeed, considered amounts of phenolic compounds such as hydrolysable and condensed tannins are considered to leach from senescent plant materials into natural water. Thus, it was possible that Fe(III) could be bound not only to aromatic substances but also phenolic/protein-like materials. This conclusion is in agreement with previous studies by Milne et al. (2003) who revealed that Ca(II) mainly bind to carboxylic-like functional groups, while Al(III) and Fe(III) were also bound to phenolic-like functional groups.

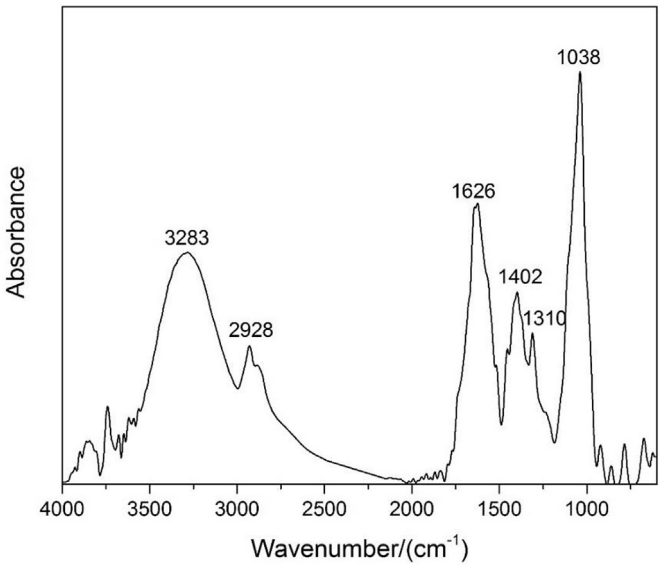

Fig. 3. The FT-IR spectrum of the freeze-dried plant-derived DOM.

However, residual metal ions Fe(III), Al(III) and Ca(II) remaining in the supernatants might affect the fluorescence intensity of DOM (Bai et al., 2008; Gao et al., 2015; Wu et al., 2011; Yan et al., 2013). Effects of metal ions on enhancement or quenching of fluorescence intensity of DOM can be large (McIntyre and Guéguen, 2013; Patel-Sorrentino et al., 2004). This might adversely affect the assessment of the concentration of the fluorescent components and result in an analytic deviation. Thus, the above conclusion based on the percentage changes of PARAFAC components should be further verified through the relationship between the fluorescence intensity and DOC concentration. Fluorescence intensity of each component was further plotted versus DOC for both raw and treated DOM samples containing different concentrations of residual metals. However, a significant relationship ($p < 0.05$) was only observed between concentrations of DOC with component 1 (Fig. 5). Changes in the percentage of component 1 could explain at least 79%, 74% and 95% of the removal of DOC by addition of Ca(II), Al(III) and Fe(III), respectively (Fig. 5). These results prompted that intensity changes of fluorescence component 1 could be, to some degree, considered as an indicator of DOM removal. Additionally, the result would also support the conclusion that Ca(II), Al(III) and Fe(III) preferentially remove humic-like and fulvic-like organic matters. However, the selective combination of Fe(III) and Al(III) with phenolic/protein-like substances needed to be verified further by orther spectroscopic methods since no significant correlation was observed between them.

Since FT-IR spectroscopy can reveal configurations of organic matter at a functional group level, organic components can be traced by comparing FT-IR peak changes (Fig. 6). Addition of Ca(II) resulted in no obvious changes of the FT-IR spectral features for the DOM remaining in the solution until its concentration reached up to 10.0 mM. The relative intensity of the peak in 1069 cm^{-1} increased when the concentration of Ca(II) was 10.0 mM, which may be due to the decrease of other peaks' intensity. The observation reveals that Ca(II) might selectively bind with organic matters such as aromatic, carboxylic-like, and amides, and also induce their precipitation in solutions. Addition of Al(III) or Fe(III) decreased all peaks' intensity of FT-IR spectra, especially peaks at 1626 cm^{-1} and 1402 cm^{-1}. This indicated that addition of Fe(III) or Al(III) caused precipitation of DOM including all C functional groups, especially for aromatic, carboxylic-like and phenolic substances.

Changes in FT-IR spectral features could be analyzed further semi-quantitatively by monitoring the ratio changes of the FT-IR peak areas. Aliphatic and carboxylic groups are two prominent components in DOM. Absorbance bands in the ranges of 3020 to 2800 cm^{-1} and 1720 to 1600 cm^{-1} in FT-IR spectra have been attributed to these two groups, respectively (He and Zhang, 2015). Two bands in the range of 3020 to 2800 cm^{-1} are grouped and designated as Band A (aliphatic), while the other band in the range of 1740 to 1600 cm^{-1} is designated as Band B (carboxylic). A band at 1100 to 1030 cm^{-1} was designated as B and C and used as a

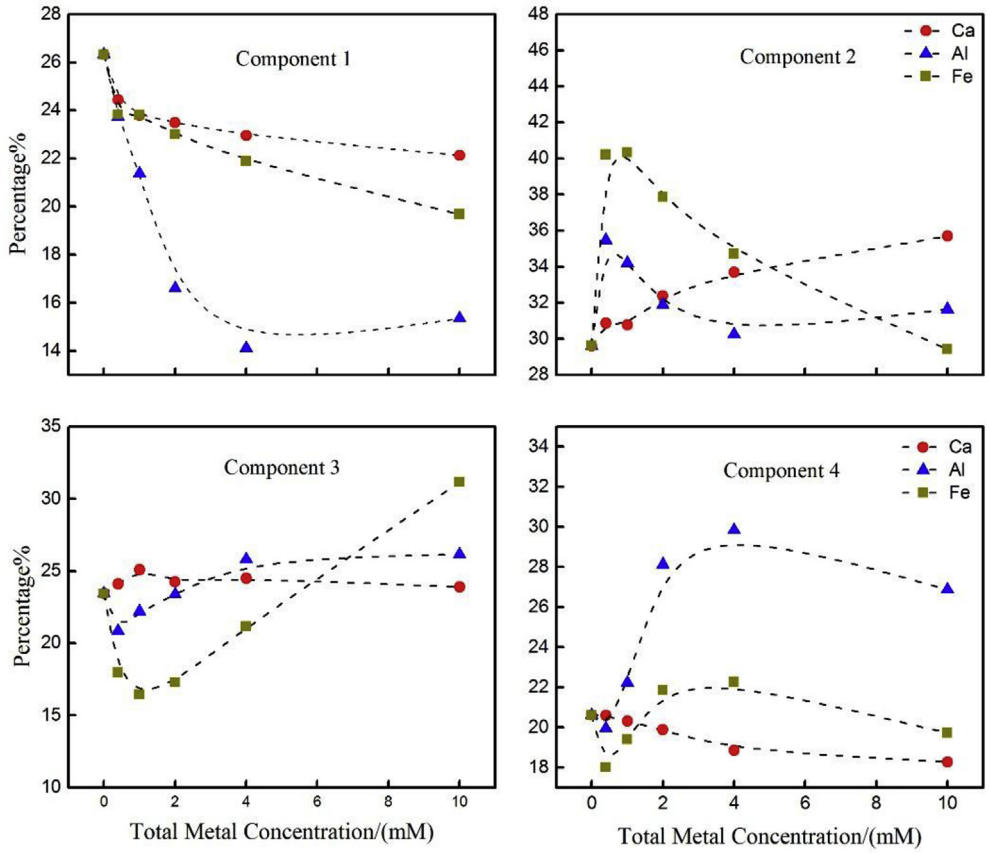

Fig. 4. Changes of the percentage of four PARAFAC components in the supernatants of plant-derived DOM extracts incubated in the presence of metal ions for coagulation.

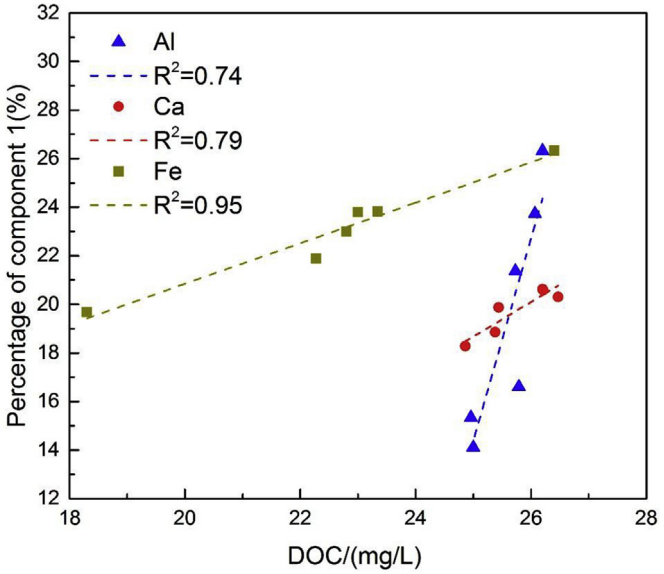

Fig. 5. Relationships between percentage of component 1 and DOC in the plant-derived DOM extracts and its supernatants after incubation in the presence of Fe(III), Al(III) and Ca(II). Dashed lines in the plot are linear regression between the two variables ($p < 0.05$).

reference for comparing the relative intensities of Bands A and B (He and Zhang, 2015). Ratios of Band A/Band C and Band B/Band C decreased when the concentration of Ca(II) was 10.0 mM (Table S1). This indicated that relative intensity around 2928 cm^{-1} and 1624 cm^{-1} decreased as a function of increasing concentration of Ca(II). These changes further confirmed that Ca(II) could bind with aliphatic and carboxyl-like compounds, and also cause their precipitation in solutions. Spectra of freeze-dried DOM remaining in supernatants after adding Al(III) or Fe(III) showed more complicate changes (Table S1). With increasing concentrations of Al(III), relative intensity of 3283 cm^{-1} and 2928 cm^{-1} decreased until the concentration of Al(III) reached up to 2.0 mM. However, a further increase in concentration of Al(III) did not further decrease, rather increased, their relative peak intensity. A similar phenomenon was observed for addition of Fe(III). This result might be caused by the substantially decrease of the normalized peak of Band C at 1038 cm^{-1} when excessive Al(III) and Fe(III) added to DOM. The presence of a peak at 1038 cm^{-1} was attributed to polysaccharide C-O stretching, silicate vibrations or P compounds (Agnelli et al., 2000; Francioso et al., 1996; He et al., 2006). For plant-derived DOM, polysaccharides or P compounds seem to have more contributions to band intensities in this region (Liu et al., 2016a). Thus, the decrease in intensity of the band at 1038 cm^{-1} might be attributable to removal of polysaccharides and P compounds. However, previous studies revealed that polysaccharides were not coagulated following additions of hydrolyzing metal salts (Masion et al., 2000). Thus, the P compound ubiquitous in plant-derived DOM might be combined with Al(III) or Fe(III) in the form of phosphate-DOM-Fe(Al) (Zhu et al., 2015), which decreased the spectral intensity around 1038 cm^{-1}. Another possible explanation might be that high concentrations of Al(III) and Fe(III) induced a decline in the adsorption-bridging capability of flocculated P-DOM-Fe(Al) polymer (Subramanian et al., 1999; Zhu et al., 2014). Thus,

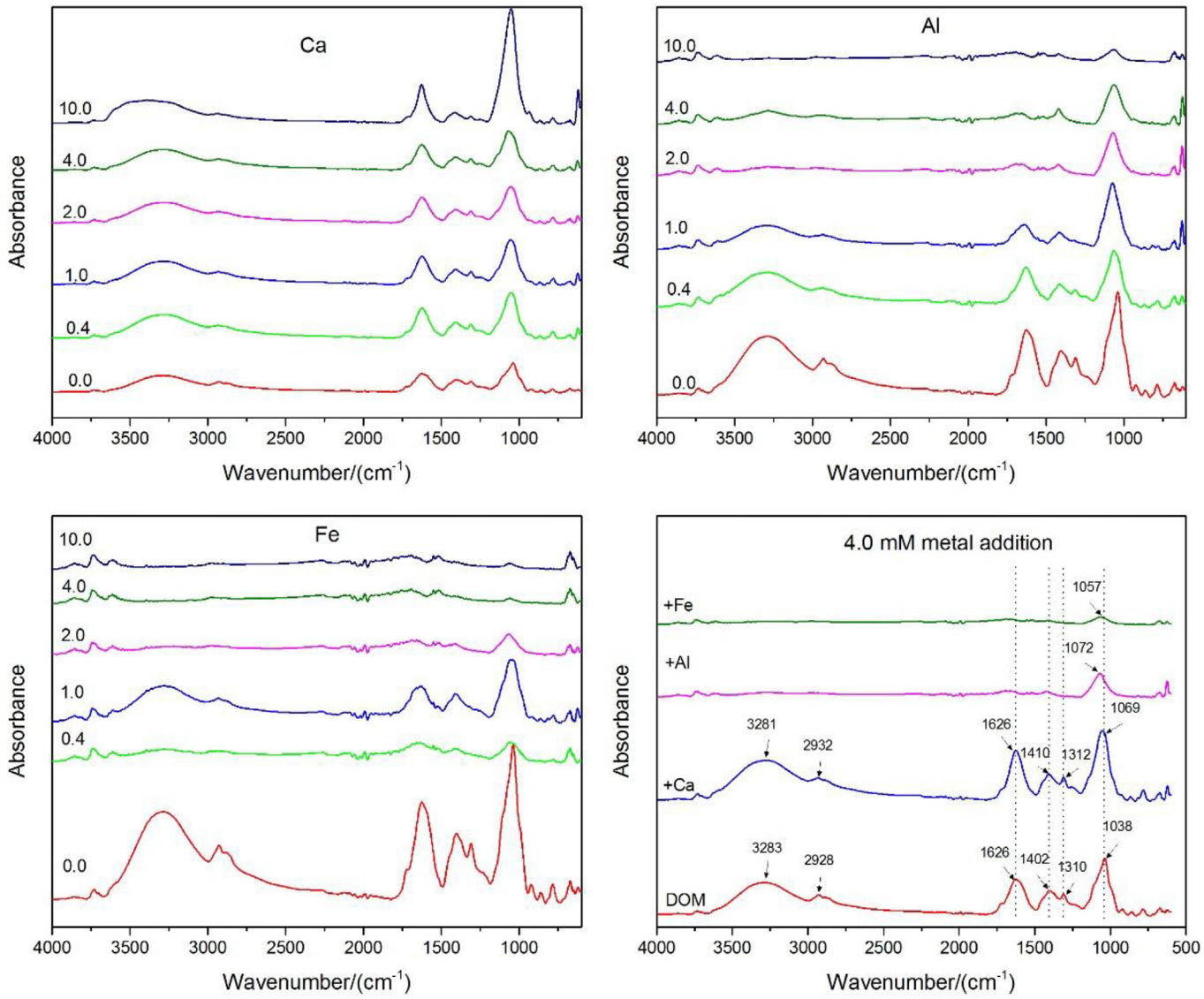

Fig. 6. FT-IR spectra of freeze-dried supernatants of plant-derived DOM extracts incubated in the presence of metals. Total metal concentrations were 0.0, 0.4, 1.0, 2.0, 4.0 and 10.0 mM, respectively.

high concentrations of Al(III) or Fe(III) would induce the excessive of soluble monomeric and possible polynuclear forms, and finally result in a decrease in net removal of DOM. In conclusion, these results revealed that both carboxylic-like substances and phosphorus in plant-derived DOM could be partly removed by interaction with Fe(III) or Al(III).

3.4. Spectral characterization of coagulated plant-derived DOM

Coagulated materials formed after addition of Ca(II), Fe(III), or Al(III) were collected, freeze-dried and further analyzed by FT-IR spectroscopy (Fig. 7). The spectrum of DOM coagulated with Ca(II) ion exhibited sharp peaks at 1614 cm^{-1} and 1321 cm^{-1}, which correspond to carboxylic-like functional groups and aromatic primary and second amines respectively. Results indicated that interactions of Ca(II) with carboxylic-like, aromatic, and amines were responsible for DOM coagulation, which is also consistent with observations from FT-IR spectra of DOM remaining in the supernatant. FT-IR spectra of DOM coagulated by Al(III) or Fe(III) exhibited three bands at 1641/1643 cm^{-1}, 1423/1414 cm^{-1}, and 1082/1067 cm^{-1} and a broad minor peak at 3333/3279 cm^{-1}. This likely indicated that Fe(III) and Al(III) cations precipitated carboxylic-like, aromatic, and phenolic-like compounds, as well as presumably P compound. These findings were consistent with results from FT-IR spectra of DOM in the supernatant and also consistent with previous report by Milne et al. (2003) who showed that Ca(II) mainly interacted with carboxylic-like functional groups of humic acid, while Fe(III) and Al(III) were also bound to phenolic-like functional groups.

3.5. Significance

Precipitation of DOM is an important biogeochemical process, which influences molecular compositions and ultimate fate of DOM in lake ecosystems. Overall, results from this study showed that aromatic, carboxylic-like, phenolic and amides compounds in organic matters could preferentially bind with metal cations and subsequently precipitate out of water. Humic organic matters with high aromaticity tended to precipitate and so accumulate in sediments. Whereas, non-humic materials such as fresh plant leachate

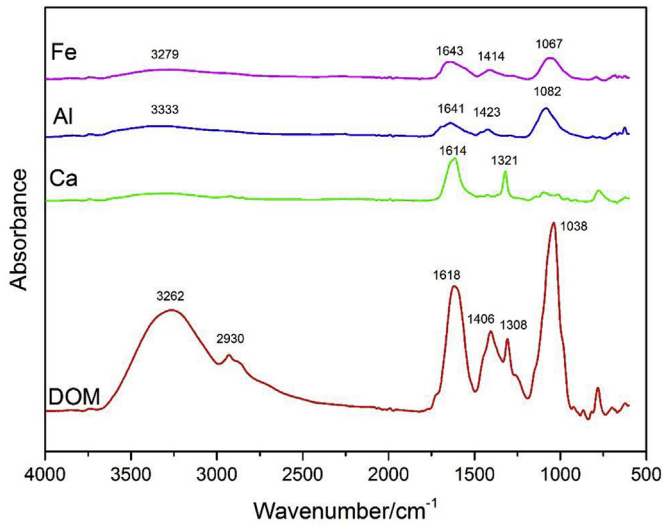

Fig. 7. FT-IR spectra of coagulated DOM induced by metal ions additions.

with lesser aromaticity would be difficult to precipitate, thus would play an important role for life in natural waters of lakes. Plant-derived DOM might have long lasting impact on water quality and organisms due to its poor coagulation with metal cations in lake ecosystems.

Coagulation or precipitation of DOM was partially determined by metal cations. This implied that the inorganic chemistry of aquatic systems has a significant effect on the cycling of organic matter. In waters of greater calcium hardness, carboxylic-like, aromatic and amines compounds likely coagulate and precipitate due to their interaction with great concentrations of Ca ions, while aromatic, phenolic, carboxylic-like and P-containing organic compounds may decrease in aquatic environment with elevated concentrations of Fe and Al cations. There are more aromatic carbon groups in sediments compared to that in water bodies such as Tai Lake (Liu et al., 2016a), which can be explained, in some degree, by the readily precipitation of aromatics with metal cations.

Insights gained from this study are also beneficial for wastewater treatment. Plant-derived DOM has a low amount of aromatics (Liu et al., 2016a, 2016b), which is likely removed with difficulty by cation-induced coagulation. On the other hand, wastewater dominated by plant leachate is difficult to remove by metal salt flocculation treatment so that this type of wastewater should be treated by biodegradation (e.g. biofiltration) or other chemical treatment (e.g. peroxidation). Thus, more appropriate measures should be taken for better wastewater treatment managements according to the specific characteristics and sources of wastewater.

4. Conclusions

Cation-induced coagulation of plant-derived DOM with Ca(II), Al(III) and Fe(III) was studied by use of EEM-PARAFAC and FT-IR spectroscopy. Coagulation by the three metals cations varied due to their different affinities to plant-derived DOM. Coagulation capabilities by Fe(III) or Al(III) was greater than that of Ca. Furthermore, molecular fractionation of plant-derived DOM was observed after coagulation by Ca(II), Fe(III) or Al(III). Both aromatic and carboxylic-like organic matters could be removed by either Ca(II), Al(III) or Fe(III) ions. Whereas amides in organic matters were preferentially removed by Ca(II), and phenolic materials were selectively removed by Fe(III) or Al(III). This observation implies that inorganic chemistry characteristics have a significant effect on composition of DOM in the overlying water of lakes. Also, plant-derived DOM would play an important role in aquatic systems due to its poor coagulation capacities compared with humic substances.

Acknowledgements

The work was supported by the National Natural Science Foundation of China (No. 41630645, 41403094 and 41573126), and China Postdoctoral Science Foundation Funded Project (No. 2017M622280 and 2016M591227).

Appendix A. Supplementary data

Supplementary data related to this article can be found at https://doi.org/10.1016/j.envpol.2017.11.076.

References

Agnelli, A., Celi, L., Degl'Innocenti, A., Corti, G., Ugolini, F., 2000. Chemical and spectroscopic characterization of the humic substances from sandstone-derived rock fragments. Soil Sci. 165, 314–327.
Amirsardari, Y., Yu, Q., Williams, P., 1997. Effects of ozonation and coagulation on turbidity and TOC removal by simulated direct filtration for potable water treatment. Environ. Technol. 18, 1143–1150.
Baghoth, S., Sharma, S., Amy, G., 2011. Tracking natural organic matter (NOM) in a drinking water treatment plant using fluorescence excitation–emission matrices and PARAFAC. Water Res. 45, 797–809.
Bai, Y., Wu, F., Liu, C., Li, W., Guo, J., Fu, P., et al., 2008. Ultraviolet absorbance titration for determining stability constants of humic substances with Cu (II) and Hg (II). Anal. Chim. Acta 616, 115–121.
Baker, A., 2001. Fluorescence excitation–emission matrix characterization of some sewage-impacted rivers. Environ. Sci. Technol. 35, 948–953.
Baker, A., Inverarity, R., 2004. Protein-like fluorescence intensity as a possible tool for determining river water quality. Hydrol. Process 18, 2927–2945.
Bernier, M.-H., Levy, G.J., Fine, P., Borisover, M., 2013. Organic matter composition in soils irrigated with treated wastewater: FT-IR spectroscopic analysis of bulk soil samples. Geoderma 209–210, 233–240.
Castillo, C.R., Sarmento, H., Álvarez-Salgado, X.A., Gasol, J.M., Marraséa, C., 2010. Production of chromophoric dissolved organic matter by marine phytoplankton. Limnol. Oceanogr. 55, 446–454.
Chen, W., Westerhoff, P., Leenheer, J.A., Booksh, K., 2003. Fluorescence excitation-emission matrix regional integration to quantify spectra for dissolved organic matter. Environ. Sci. Technol. 37, 5701–5710.
Christl, I., Kretzschmar, R., 2007. C-1s NEXAFS spectroscopy reveals chemical fractionation of humic acid by cation-induced coagulation. Environ. Sci. Technol. 41, 1915–1920.
Coble, P.G., 1996. Characterization of marine and terrestrial DOM in seawater using excitation-emission matrix spectroscopy. Mar. Chem. 51, 325–346.
Cuss, C., Guéguen, C., 2015. Characterizing the labile fraction of dissolved organic matter in leaf leachates: methods, indicators, structure, and complexity. In: He, Z., Wu, F. (Eds.), Labile Organic Matter—Chemical Compositions, Function, and Significance in Soil and the Environment. Soil Science Society of America, Madison, pp. 237–274.
Duarte, R.M., Pio, C.A., Duarte, A.C., 2005. Spectroscopic study of the water-soluble organic matter isolated from atmospheric aerosols collected under different atmospheric conditions. Anal. Chim. Acta 530, 7–14.
Findlay, S., Sinsabaugh, R.L., 2003. Aquatic Ecosystems: Interactivity of Dissolved Organic Matter. Academic Press.
Francioso, O., Sanchez-Cortes, S., Tugnoli, V., Ciavatta, C., Sitti, L., Gessa, C., 1996. Infrared, raman, and nuclear magnetic resonance (^{1}H, ^{13}C, and ^{31}P) spectroscopy in the study of fractions of peat humic acids. Appl. Spectrosc. 50, 1165–1174.
Fu, P., Wu, F., Liu, C., Wang, F., Li, W., Yue, L., et al., 2007. Fluorescence characterization of dissolved organic matter in an urban river and its complexation with Hg (II). Appl. Geochem. 22, 1668–1679.
Gao, Y., Yan, M., Korshin, G., 2015. Effects of calcium on the chromophores of dissolved organic matter and their interactions with copper. Water Res. 81, 47–53.
Gone, D.L., Seidel, J.-L., Batiot, C., Bamory, K., Ligban, R., Biemi, J., 2009. Using fluorescence spectroscopy EEM to evaluate the efficiency of organic matter removal during coagulation–flocculation of a tropical surface water (Agbo reservoir). J. Hazard. Mater. 172, 693–699.
He, Z., Honeycutt, C., Griffin, T., 2003. Comparative investigation of sequentially extracted phosphorus fractions in a sandy loam soil and a swine manure. Commun. Soil Sci. Plant Anal. 34, 1729–1742.
He, Z., Ohno, T., Cade-Menun, B.J., Erich, M.S., Honeycutt, C.W., 2006. Spectral and chemical characterization of phosphates associated with humic substances Soil Sci. Soc. Am. J. 70, 1741–1751.
He, Z., Uchimiya, M., Cao, H., 2014. Intrinsic fluorescence excitation–emission matrix spectral features of cottonseed protein fractions and the effects of

denaturants. J. Am. Oil Chem. Soc. 91, 1489–1497.
He, Z., Zhang, M., 2015. Structural and functional comparison of mobile and recalcitrant humic fractions from agricultural soils. In: He, Z., Wu, F. (Eds.), Labile Organic Matter—Chemical Compositions, Function, and Significance in Soil and the Environment. Soil Science Society of America, Madison, pp. 79–98.
Hernes, P.J., Bergamaschi, B.A., Eckard, R.S., Spencer, R.G., 2009. Fluorescence-based proxies for lignin in freshwater dissolved organic matter. J. Geophys. Res. Biogeosci. 114.
Ishii, S.K.L., Boyer, T.H., 2012. Behavior of reoccurring PARAFAC components in fluorescent dissolved organic matter in natural and engineered systems: a critical review. Environ. Sci. Technol. 46, 2006–2017.
Kaiser, K., 1998. Fractionation of dissolved organic matter affected by polyvalent metal cations. Org. Geochem. 28, 849–854.
Kang, K.-H., Shin, H.S., Park, H., 2002. Characterization of humic substances present in landfill leachates with different landfill ages and its implications. Water Res. 36, 4023–4032.
Kerndorff, H., Schnitzer, M., 1980. Sorption of metals on humic acid. Geochim. Cosmochim. Acta 44, 1701–1708.
Lawaetz, A.J., Stedmon, C.A., 2009. Fluorescence intensity calibration using the Raman scatter peak of water. Appl. Spectrosc. 63, 936–940.
Lguirati, A., Ait Baddi, G., El Mousadik, A., Gilard, V., Revel, J.C., Hafidi, M., 2005. Analysis of humic acids from aerated and non-aerated urban landfill composts. Int. Biodeter. Biodegr. 56, 8–16.
Li, W.-H., Sheng, G.-P., Liu, X.-W., Yu, H.-Q., 2008. Characterizing the extracellular and intracellular fluorescent products of activated sludge in a sequencing batch reactor. Water Res. 42, 3173–3181.
Liu, S., Zhu, Y., Meng, W., He, Z., Feng, W., Zhang, C., et al., 2016a. Characteristics and degradation of carbon and phosphorus from aquatic macrophytes in lakes: insights from solid-state ^{13}C NMR and solution ^{31}P NMR spectroscopy. Sci. Total Environ. 543, 746–756.
Liu, S., Zhu, Y., Wu, F., Meng, W., He, Z., Giesy, J.P., 2016b. Characterization of plant-derived carbon and phosphorus in lakes by sequential fractionation and NMR spectroscopy. Sci. Total Environ. 566, 1398–1409.
Liu, S., Zhu, Y., Wu, F., Meng, W., Wang, H., He, Z., et al., 2017. Using solid ^{13}C NMR coupled with solution ^{31}P NMR spectroscopy to investigate molecular species and lability of organic carbon and phosphorus from aquatic plants in Tai Lake, China. Environ. Sci. Pollut. Res. 24, 1880–1889.
Maie, N., Scully, N.M., Pisani, O., Jaffé, R., 2007. Composition of a protein-like fluorophore of dissolved organic matter in coastal wetland and estuarine ecosystems. Water Res. 41, 563–570.
Masion, A., Vilgé-Ritter, A., Rose, J., Stone, W.E., Teppen, B.J., Rybacki, D., et al., 2000. Coagulation-flocculation of natural organic matter with Al salts: speciation and structure of the aggregates. Environ. Sci. Technol. 34, 3242–3246.
McIntyre, A.M., Guéguen, C., 2013. Binding interactions of algal-derived dissolved organic matter with metal ions. Chemosphere 90, 620–626.
Milne, C.J., Kinniburgh, D.G., Van Riemsdijk, W.H., Tipping, E., 2003. Generic NICA–Donnan model parameters for metal-ion binding by humic substances. Environ. Sci. Technol. 37, 958–971.
Murphy, K.R., Hambly, A., Singh, S., Henderson, R.K., Baker, A., Stuetz, R., et al., 2011. Organic matter fluorescence in municipal water recycling schemes: toward a unified PARAFAC model. Environ. Sci. Technol. 45, 2909–2916.
Nierop, K.G., Jansen, B., Verstraten, J.M., 2002. Dissolved organic matter, aluminium and iron interactions: precipitation induced by metal/carbon ratio, pH and competition. Sci. Total Environ. 300, 201–211.
Ohno, T., He, Z., 2011. Fluorescence spectroscopic analysis of organic matter fractions: the current status and a tutorial case study. In: He, Z. (Ed.), Environmental Chemistry of Animal Manure. Nova Science Publishers, Hauppauge, NY, pp. 83–103.
Olk, D.C., Brunetti, G., Senesi, N., 2000. Decrease in humification of organic matter with intensified lowland rice cropping a wet chemical and spectroscopic investigation. Soil Sci. Soc. Am. J. 64, 1337–1347.
Osburn, C.L., Handsel, L.T., Mikan, M.P., Paerl, H.W., Montgomery, M.T., 2012. Fluorescence tracking of dissolved and particulate organic matter quality in a river-dominated estuary. Environ. Sci. Technol. 46, 8628–8636.
Patel-Sorrentino, N., Mounier, S., Lucas, Y., Benaim, J., 2004. Effects of UV–visible irradiation on natural organic matter from the Amazon basin. Sci. Total Environ. 321, 231–239.
Riedel, T., Biester, H., Dittmar, T., 2012. Molecular fractionation of dissolved organic matter with metal salts. Environ. Sci. Technol. 46, 4419–4426.
Romera-Castillo, C., Sarmento, H., Álvarez-Salgado, X.A., Gasol, J.M., Marrasé, C., 2011. Net production and consumption of fluorescent colored dissolved organic matter by natural bacterial assemblages growing on marine phytoplankton exudates. Appl. Environ. Microb. 77, 7490–7498.
Senesi, N., 1990. Molecular and quantitative aspects of the chemistry of fulvic acid and its interactions with metal ions and organic chemicals: Part II. The fluorescence spectroscopy approach. Anal. Chim. Acta 232, 77–106.
Stedmon, C.A., Bro, R., 2008. Characterizing dissolved organic matter fluorescence with parallel factor analysis: a tutorial. Limnol. Oceanogr. Methods 6, 572–579.
Stedmon, C.A., Markager, S., 2005. Tracing the production and degradation of autochthonous fractions of dissolved organic matter by fluorescence analysis. Limnol. Oceanogr. 50, 1415–1426.
Subramanian, R., Zhu, S., Pelton, R., 1999. Synthesis and flocculation performance of graft and random copolymer microgels of acrylamide and diallyldimethylammonium chloride. Colloid Polym. Sci. 277, 939–946.
Swietlik, J., Sikorska, E., 2006. Characterization of natural organic matter fractions by high pressure size-exclusion chromatography, specific UV absorbance and total luminescence spectroscopy. Pol. J. Environ. Stud. 15, 145.
Tipping, 2002. Cation Binding by Humic Substances, vol. 12. Cambridge University Press.
Wu, F., Cai, Y., Evans, D., Dillon, P., 2004a. Complexation between Hg(II) and dissolved organic matter in stream waters: an application of fluorescence spectroscopy. Biogeochemistry 71, 339–351.
Wu, F., Evans, R., Dillon, P., 2003. Separation and characterization of NOM by high-performance liquid chromatography and on-line three-dimensional excitation emission matrix fluorescence detection. Environ. Sci. Technol. 37, 3687–3693.
Wu, F., Mills, R., Evans, R., Dillon, P., 2004b. Kinetics of metal– fulvic acid complexation using a stopped-flow technique and three-dimensional excitation emission fluorescence spectrophotometer. Anal. Chem. 76, 110–113.
Wu, F., Xing, B., 2009. Natural Organic Matter and its Significance in the Environment. Science Press.
Wu, J., Zhang, H., He, P.-J., Shao, L.-M., 2011. Insight into the heavy metal binding potential of dissolved organic matter in MSW leachate using EEM quenching combined with PARAFAC analysis. Water Res. 45, 1711–1719.
Yamashita, Y., Tanoue, E., 2003. Chemical characterization of protein-like fluorophores in DOM in relation to aromatic amino acids. Mar. Chem. 82, 255–271.
Yan, M., Benedetti, M.F., Korshin, G.V., 2013. Study of iron and aluminum binding to Suwannee River fulvic acid using absorbance and fluorescence spectroscopy: comparison of data interpretation based on NICA-Donnan and Stockholm humic models. Water Res. 47, 5439–5446.
Yan, M., Korshin, G.V., 2014. Comparative examination of effects of binding of different metals on chromophores of dissolved organic matter. Environ. Sci. Technol. 48, 3177–3185.
Zhang, Y., Liu, X., Wang, M., Qin, B., 2013. Compositional differences of chromophoric dissolved organic matter derived from phytoplankton and macrophytes. Org. Geochem. 55, 26–37.
Zhao, A., Zhang, M., He, Z., 2013. Spectroscopic characteristics and biodegradability of cold and hot water–extractable soil organic matter under different land uses in subarctic Alaska. Commun. Soil Sci. Plant Anal. 44, 3030–3048.
Zhu, G., Yin, J., Zhang, P., Wang, X., Fan, G., Hua, B., et al., 2014. DOM removal by flocculation process: fluorescence excitation–emission matrix spectroscopy (EEMs) characterization. Desalination 346, 38–45.
Zhu, Y., Wu, F., He, Z., Giesy, J.P., Feng, W., Mu, Y., et al., 2015. Influence of natural organic matter on the bioavailability and preservation of organic phosphorus in lake sediments. Chem. Geol. 397, 51–60.

Cation-induced coagulation of aquatic plant-derived dissolved organic matter: investigation by EEM-PARAFAC and FT-IR spectroscopy

Shasha Liu [a,b], Yuanrong Zhu [b], Leizhen Liu [c], Zhongqi He [d], John P. Giesy [e], Yingchen Bai [b], Fuhong Sun [b,*], Fengchang Wu [b]

[a] Key Laboratory of Marine Environment and Ecology, Ministry of Education, Ocean University of China, Qingdao 266100, China

[b] State Key Laboratory of Environment Criteria and Risk Assessment, Chinese Research Academy of Environmental Sciences, Beijing 100012, China

[c] Faculty of Geographical Science, Beijing Normal University, Beijing 100875, China.

[d] USDA-ARS Southern Regional Research Center, 1100 Robert E Lee Blvd, New Orleans, LA 70124, USA

[e] Department of Veterinary Biomedical Sciences and Toxicology Centre, University of Saskatchewan, Saskatoon, Saskatchewan S7N 5B3, Canada

*** Corresponding author (Fuhong Sun).**

Mailing address: No. 8 Dayangfang, BeiYuan Road, ChaoYang District, Beijing, 100012, China;

E-mail address: sunfhiae@126.com

Table S1. Ratios of FT-IR band integral area of freeze-dried supernatants of plant-derived DOM extracts incubated in the presence of metal ions. Band A (aliphatic, 3020 to 2800 cm^{-1}), Band B (carboxylic, 1740 to 1600 cm^{-1}), Band C (carbohydrates or P compounds, 1100 to 1030 cm^{-1})

Group	Concentration/mM	Band A/Band C	Band B/Band C	Band A/Band B
Ca(II)	0	0.14	1.02	0.14
	0.4	0.07	0.87	0.08
	1	0.07	0.85	0.08
	2	0.07	1.00	0.07
	4	0.06	0.89	0.07
	10	0.02	0.35	0.05
Al(III)	0	0.14	1.02	0.14
	0.4	0.07	0.89	0.08
	1	0.05	0.58	0.09
	2	0.04	0.87	0.05
	4	0.07	0.90	0.07
	10	0.18	4.36	0.04
Fe(III)	0	0.14	1.02	0.14
	0.4	0.16	3.15	0.05
	1	0.08	1.10	0.07
	2	0.10	2.87	0.04
	4	0.79	22.04	0.04
	10	0.67	18.82	0.04

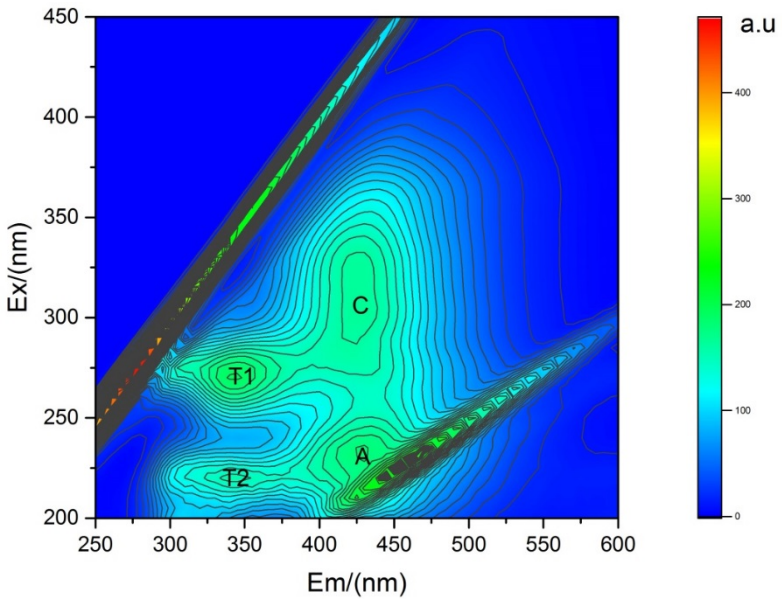

Fig. S1. Fluorescence EEM spectrum of the plant-derived DOM. Peak C, visible humic-like fluorescence peak; Peak A, ultraviolet humic-like fluorescence peak; Peak T1, visible protein-like fluorescence peaks; Peak T2, ultraviolet protein-like fluorescence peaks.